

ONLINE OPTIMIZATION OF NSLS-II DYNAMIC APERTURE AND INJECTION TRANSIENT*

X. Yang[†], G. Wang, V. Smaluk, L. H. Yu, T. Shaftan, Y. Li, F. Plassard, S. Buda, Y. Hidaka, D. Durfee, Y. Tian, Y. Hu, K. Ha, A. Derbenev, B. Bacha, C. Danneil, D. Padrazo
National Synchrotron Light Source II, Brookhaven National Laboratory, Upton, NY, USA

Abstract

The goal of the NSLS-II online optimization project is to improve the beam quality for the user experiments. To increase the beam lifetime and injection efficiency, we have developed a model-independent online optimization of nonlinear beam dynamics using advanced algorithms, such as Robust Conjugate-Gradient Algorithm (RCDS). The optimization objective is the injection efficiency and optimization variables are the sextupole magnet strengths. Using the online optimization technique, we increased the NSLS-II dynamic aperture and reduced the amplitude-dependent tune shift. Recently, the sextupole optimization was successfully applied to double the injection efficiency up to above 90% for the high-chromaticity lattice being developed to improve the beam stability and to increase the single-bunch beam intensity. Minimizing the beam perturbation during injection is the second objective in this project, realized by online optimization of the injection kickers. To optimize the full set of kicker parameters, including the trigger timing, amplitude, and pulse width, we upgraded all kicker power supplies with the capability of tunable waveform width. As a result, we have reduced the injection transient by a factor of 29, down to the limit of 60 μm .

INTRODUCTION

The Facility Improvement Project “Methods of online optimization of NSLS-II storage ring concurrent with user operations” was dedicated to developing a set of software tools for online optimization of beam dynamics and minimization of the injection transients. The online optimization approach is based on the use of the measured beam and machine parameters to evaluate performance functions, which are optimized using advanced algorithms designed to work reliably in noisy environments.

In the frameworks of this project, we planned to explore and improve the performance of the optimization algorithms. We use beam-based model-independent online methods to improve the injection efficiency and beam lifetime by direct optimization of sextupoles. For the minimization of the injection transients [1-4], the specific plan was to optimize the matching of Storage Ring (SR) injection kickers [5-7].

We expect the NSLS-II user community to benefit from the reduced top-off injection frequency, improved beam stability, and transparent injection. Since nonlinear beam dynamics is a subject of high scientific interest, we believe the results of this project will be beneficial not only for NSLS-II but also for other present and future light sources.

* This manuscript has been authored by Brookhaven Science Associates, LLC under Contract No. DE-SC0012704 with the U.S. DOE

[†] xiyang@bnl.gov

STUDY RESULTS

Optimization of Sextupoles to Increase DA

To test the RCDS optimization algorithm [8], we loaded the high chromaticity 7 lattice. The injection efficiency was decreased to around 20%. The RCDS online optimization of sextupoles recovered the injection efficiency up to 90% at the second iteration. In this experiment, we found two to three iterations were adequate to achieve the optimal solution. Extra iterations were not so effective, the injection efficiency went from mild improvement to no improvement at all. The evolution of the power supply currents of the NSLS-II sextupole families is shown in the right plot of Fig. 1.

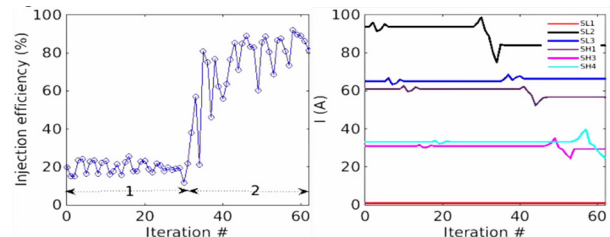


Figure 1: Two iterations of the RCDS online optimization of sextupoles for the high chromaticity 7 lattice: injection efficiency (left) and the sextupole settings (right).

We characterized the dynamic aperture (DA) for the NSLS-II operational lattice. We injected a beam of 2 mA current in 50 bunches, which were well aligned on the flat top of the pinger pulse. Then, we gradually increased the pinger voltage and recorded the beam current measured by the DCCT. Figure 2 shows the horizontal (left) and vertical (right) DA before (red) and after (blue) RCDS online optimization. We have achieved a more than 20% increase in the horizontal DA with no change in the vertical DA. We also analysed the measured betatron tune shift with amplitude and observed a reduction of the horizontal tune shift with amplitude by a factor of two.

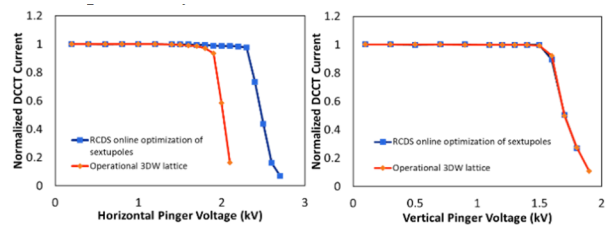


Figure 2: Horizontal (left) and vertical (right) DA before (red) and after (blue) sextupole optimization in the 3DW lattice.

We successfully applied the sextupole optimization to the lattice with high chromaticity, +7, in both horizontal

and vertical directions. High chromaticity provides fast damping of betatron oscillations allowing us to reduce the bunch-by-bunch feedback gain. This helps to improve the beam size stability in the operations with small vertical emittance. High chromaticity is also useful to increase the single-bunch beam intensity, so the other application of this lattice is the new operation mode with high-intensity bunches for time-resolved experiments.

Minimization of the Injection Transient

For the injection, four pulse kickers create a horizontal orbit bump in the injection straight section [6,7]. The orbit outside the bump is unperturbed if the kickers are perfectly matched. Any mismatch of the kicker pulses results in the residual beam oscillation around the ring perturbing the user beam. The online optimization was applied to provide the top-off injection with minimized perturbations of the beamline user operations. Optimizing the matching of four injection kickers helps to reduce the perturbation of the stored beam orbit and achieve a more transparent injection.

Initially, all the kickers were set to the operational values with the same kicker amplitude. We did the optimization in three steps with different combinations of the knobs [9]. First, we varied amplitudes of 3 kickers and monitored the residual betatron oscillation during the injection in one fixed RF bucket. This step showed very fast convergence (within one hour) and minimized the injection transient from 1.2 mm down to 0.15-0.2 mm peak-to-peak, which is dominated by the kicker shot-to-shot variation. Then, with the optimized kicker amplitudes, we varied the timing delays of 3 kickers and repeated the same optimization process. As predicted, these two steps worked very well to minimize the injection transient of a certain injected bunch, but other bunches in the train still have a large transient. In the last step, we varied both amplitude and timing with excitation of all the bunches from 0 to 1000 with a step of 100, in the same way as the top-off injection. The objective function is the average RMS value of each bunch. Although the knobs were set close to the optimal values after the first two steps, the optimization took a much longer time, about 4 hours, to reach the minimum. We observed a dependence of the residual oscillation on the number of the injection bucket, illustrated by Fig. 3.

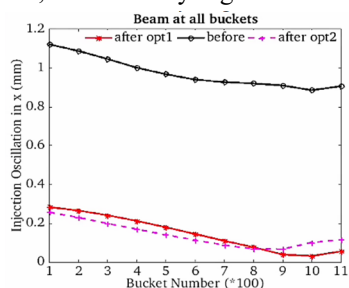


Figure 3: RMS value of BPM turn-by-turn data vs the injection bucket: before optimization (black), after optimization of the first 20 buckets (red), after global optimization of 1000 buckets (magenta).

The RMS values of the measured oscillations are shown before the optimization (black), after the optimization with the first 20 buckets filled with 1.6 mA (red), and after the

global optimization of 1000 buckets filled with 22 mA (magenta). The global optimization of the pulse amplitude and timing of the injection kickers reduces the injection transient by a factor of six from 1.2 mm down to 0.2 mm.

Reduction of Timing Jitter

The timing jitter caused by the timing system only should be smaller than 15 ps. Using the event generator transistor-to-transistor logic output channels providing the triggers for the injection kickers, we confirmed that the jitter is mainly caused by the kicker system itself.

The time jitters of all 4 injection kickers were similar, about 2 ns in RMS and 4-5 ns in FWHM depending on where the measurement was performed. A smaller jitter of about 4 ns was measured right at the pulser, and jitter of 5 ns was measured after the delay line. Each kicker has 10 IGBTs connected in series and triggered by fiber optical receivers. Based on the diagnostic measurements, we concluded the time jitter comes from the fiber optics receiver. A new trigger board was designed, manufactured, and tested. It provides a significant reduction of the timing jitter by a factor of 10, from 2 ns down to 200 ps. For each of the 4 SR injection kickers, 11 boards (1 master fan-out and 10 stage trigger boards) are needed. All 44 trigger boards were replaced sequentially during the maintenance days in May-June 2019. The performance was evaluated before and after the installation of new trigger boards by analysis of 180 kicker waveforms to extract the timing and amplitude jitters:

- A reference waveform is obtained by averaging 180 injections.
- Each waveform is subtracted from the reference waveform.

After the installation of new trigger boards for injection kicker 1, 180 waveforms were taken for all 4 kickers. The processed data show the cosine-like patterns for kickers 2, 3, and 4, which indicates the timing jitter of these kickers, except kicker 1. To extract the timing jitters, the cosine-like patterns were normalized by $(\text{amplitude} \cdot \omega)$ [10]. As shown in Fig. 4, the timing jitter of kicker 1 is on the noise level; the timing jitters of the other three kickers are about 2 ns peak-to-peak. After the upgrade of new trigger boards for all 4 kickers, their timing jitters have gone down to the noise level, as shown in Fig. 5.

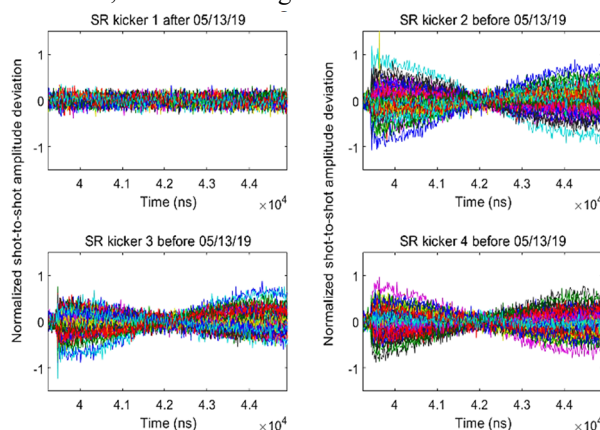


Figure 4: Data were taken at 05/13/19 with upgraded k1.

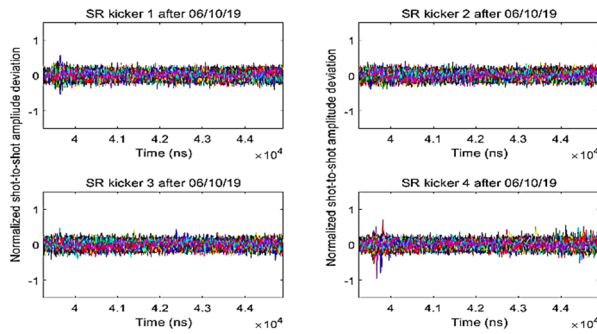


Figure 5: Kicker waveforms measured on 06/10/19 with all 4 upgraded kickers.

Implementation of Tunable Kicker Waveform

Mode analysis of the SR injection kickers provides the information of the amplitude deviation, timing offset, and waveform width deviation [10]. Four pulsers have been designed, manufactured, tested, and installed. The tuning slot is activated by a stepper motor to vary the inductance and, therefore, the width of the kicker pulse. The motion of the stepper motor is precisely controlled by the integrated motion control functions of a SIEMENS 1215C DC/DC/DC PLC. The achieved tuning range of 70 ns meets the specification with nanosecond precision, as shown in Fig. 6. Then, the associated control program was developed, tested, and installed.

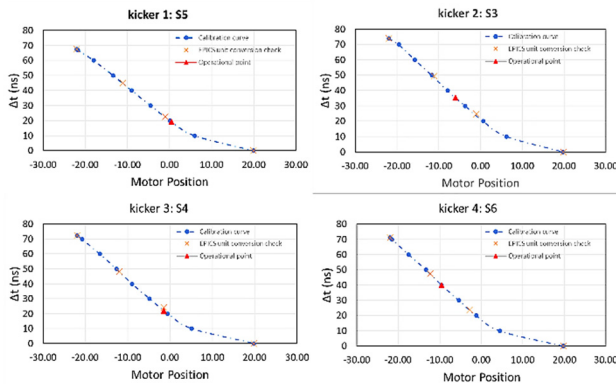


Figure 6: Unit conversions from the motor position to the variation of the kicker pulse width.

Optimization with Full Set of Kicker Parameters

The kicker hardware upgrade reduces the trigger timing jitter down to 1 ns in RMS and provides a tunable pulse width with a 1 ns precision in a range of 70 ns. The upgrade allows us to optimize the injection transient with a full set of parameters, including the amplitude, trigger timing, and pulse width of all 4 injection kickers.

However, there were some issues related to the BPM turn-by-turn readback, which distorted the measurement of injection transients. We found that the BPM turn-by-turn data had a shot-to-shot variation of the injection transient larger than usual for the RF buckets in the range of 0-300 and 800-1200. The misalignment of the BPM timing in the turn-by-turn mode was identified at the top of the list of leading causes. Then, all BPMs were realigned with respect to timing event 47 for all RF buckets from 0 to 1200. As a result, we have an improved BPM turn-by-turn

readback with a timing error significantly smaller than the duration of a bucket (2 ns). Now, the BPMs can be used as a diagnostic tool for the online optimization of the injection transient.

Figure 7 presents the results of the injection transient optimization, the RMS residual oscillations are shown as a function of the injection bucket number before (black) and after (blue) the first RCDS online optimization, after fixing the trigger timing jitter (magenta), after implementing the adjustable width of the kicker waveform (red), and after fixing the BPM alignment issue (green and cyan). With the reliable BPM turn-by-turn readback for the buckets from 1 to 1000, we have achieved the targeted injection transient of 70 μm , which is close to the ultimate limit of 60 μm determined by the design of the off-axis injection scheme [5-7].

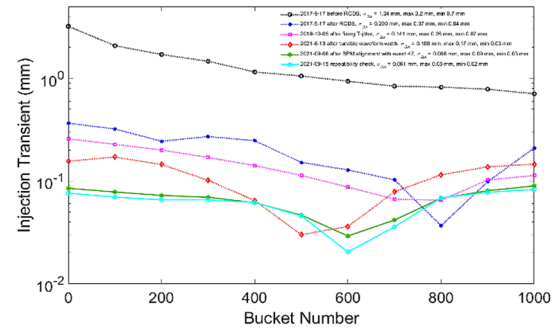


Figure 7: The measured injection transient as a function of bucket number. The injection transient is reduced to 60 μm , with the total improvement by a factor of 20.

CONCLUSION

By applying RCDS online optimization, we increased the horizontal dynamic aperture by 20% for the operational lattice. Using the same approach, we improved the injection efficiency from 40% to 90% for the newly developed lattice with high chromaticity.

Ultimately, we have minimized the injection transient by matching the injection orbit bump via online optimization of the Storage Ring injection kickers including the timing delay, pulse amplitude, and pulse width. First, we reduced the timing jitter of the injection kickers from 4-5 ns down to 1 ns by the upgrade of the fiber-optical fanout trigger boards with the new design. Then, simulation studies indicated that for the minimum injection transient of 60 μm , the pulse widths of all kickers need to be adjusted with nanosecond precision. We have completed the hardware modifications of the injection kicker power supplies and achieved the desired range of 70 ns to adjust kicker pulse width, the nanosecond tuning precision has been demonstrated too. The goal was to reduce the injection transient down to a level that would be nearly transparent to most of the beamline users, about 60 μm . We have minimized the RMS injection transient down to 70 μm , which is close to the target value. We plan a few experiments with NSLS-II beamlines to check the residual injection transient effects on the X-ray beam quality. After these final tests, the optimization results are ready to be implemented in regular user operations.

REFERENCES

- [1] J. Keil, G. Kube, F. Obier, G. K. Sahoo, and R. Wanzenberg, “Optimization of the Injection Kicker Bump Leakage at PETRA III”, in *Proc. IPAC'18*, Vancouver, Canada, Apr.-May 2018, pp. 1467-1470. doi:10.18429/JACoW-IPAC2018-TUPMF084
- [2] T. Mitsuhashi and A. Ueda, “Optimization of Kicker Pulse Bump by Using a SR Monitor at the Photon Factory”, in *Proc. PAC'05*, Knoxville, TN, USA, May 2005, paper RPAE042, p. 2717.
- [3] S. M. Liuzzo et al., “RCDS Optimizations for the ESRF Storage Ring”, in *Proc. IPAC'16*, Busan, Korea, May 2016, pp. 3420-3423. doi:10.18429/JACoW-IPAC2016-THPMR015
- [4] Y. B. Leng, Y. B. Yan, Y. Yang, R. X. Yuan, and N. Zhang, “Bunch By Bunch Transverse Beam Position Observation and Analyze During Injection at SSRF”, in *Proc. IBIC'13*, Oxford, UK, Sep. 2013, paper WEPC28, pp. 746-748.
- [5] S. Dierker, et al., “National Synchrotron Light Source II Preliminary Design Report,” <https://www.bnl.gov/isd/documents/75003.pdf>
- [6] T. V. Shafan et al., “NSLS-II Injection Concept”, in *Proc. PAC'05*, Knoxville, TN, USA, May 2005, paper RPAE058.
- [7] T. V. Shafan et al., “Status of the NSLS-II Injection System Development”, in *Proc. IPAC'10*, Kyoto, Japan, May 2010, paper WEPEA082, pp. 2672-2674.
- [8] X. Huang, J. Safranek, “Online optimization of storage ring nonlinear beam dynamics”, *PRAB* vol. 18, p. 084001, 2015.
- [9] G. M. Wang, W. X. Cheng, J. Choi, T. V. Shafan, and X. Yang, “Storage Ring Injection Kickers Alignment Optimization in NSLS-II”, in *Proc. IPAC'17*, Copenhagen, Denmark, May 2017, pp. 4683-4685. doi:10.18429/JACoW-IPAC2017-THPVA095
- [10] X. Yang, et al., “Online Optimization of NSLS-II Dynamic Aperture and Injection Transient (Facility Improvement Project)”, NSLSII-ASD-TN-372. <https://www.osti.gov/servlets/purl/1837223>